Journal of University of Science and Technology Beijing
Volume 13, Number 4, August 2006, Page 372

Materials

Effects of postthermal treatment and UV irradiation on the structure of titania-polyacrylate nanocomposites

Tao Wan [1,2], *Fei Feng*[1], *and Yuechuan Wang*[1]

1) State Key Laboratory of Polymer Materials Engineering, College of Polymer Science and Engineering, Sichuan University, Chengdu 610065, China
2) College of Materials and Chemistry & Chemical Engineering, Chengdu University of Technology, Chengdu 610059, China

(Received 2005-10-18)

Abstract: The effects of postthermal treatment and irradiation time on the structure and thermal stability of TiO_2/polyacrylate nanocomposites by a sol-gel process in reverse micelles and subsequent rapid photopolymerization were investigated, and the hybrid films were characterized by thermal gravimetry analysis (TGA), X-ray photoelectron spectrum (XPS), and atomic force microscopy (AFM). XPS data suggested that the prolongation of irradiation time and the postthermal treatment promoted titania formation, with the former affecting more remarkably. TGA data showed that TiO_2-hybrid films could upgrade the decomposition onset temperature (T_{onset}) as well as the temperature at which there is a maximum mass loss rate (T_{max}). AFM data demonstrated that the inorganic titania particles with a mean diameter of 25.26-28.84 nm were homogeneously distributed in the organic matrix.

Key words: titanium dioxide; reverse micelles; sol-gel method; photopolymerization; nanocomposites

1. Introduction

As novel functional materials, hybrid organic-inorganic nanocomposites offer the opportunity to combine the desirable properties of organic polymers (toughness, elasticity) with those of inorganic solids (hardness, chemical resistance). As the materials have been largely applied in many areas such as optics, electronics, ionics, mechanics, protective coatings, catalysis, sensors, and biology [1-4], they have received much attention in the fields of material science.

Up to now, there are only few references reporting the preparation of polymer/titania hybrid materials by the sol-gel method although titania has unique mechanical, thermal, optical, and electronic properties. Wilkes *et al.* [5] successfully prepared the high refractive-index organic-inorganic hybrid materials using titanium tetraisopropoxide as the inorganic precursor to react with triethoxysilane-capped poly(arylene ether ketone) and poly(arylene ether sulfone). Lee and Chen [6] had synthesized the high-refractive index PMMA-titania hybrid thin films, which could be potentially used as optical thin films. Hiroyo *et al.* [7] successfully prepared the photosensitive inorganic-organic hybrid films from the titanium alkoxide containing vinylpyrrolidone (VP) and the hybrid film has excellent patternability and controlled refractive index in the range between 1.8 and 2.1 after postthermal treatment between 150°C and 400°C.

However, the approach used to realize inorganic-organic nanocomposites in this study differs from the above-mentioned reports as it makes use of a sol-gel process in reverse micelles and subsequent *in situ* photopolymerization, using reactive monomer as continuous oil phase without the extraction of the synthesized nanoparticles from the transparent solution. So this research opens up a new kind of nanocomposite synthesis method, which can be applied to other inorganic-organic nanocomposites besides titania/polymer nanocomposites.

This article investigates the effects of postthermal treatment and irradiation time on the structure and thermal stability of TiO_2/polyacrylates nanocomposites, synthesized by the sol-gel process in reverse micelles and subsequent *in situ* photopolymerization. Transparent hybrid film with a tunable refractive index of 1.46-1.52 and small shrinkage can be potentially used as the holographic recording materials.

2. Materials and methods

2.1. Materials

Butyl acrylate (BA), chemical grade, was washed with 30wt% NaOH solution thrice. Acrylic acid (AA), analytical grade, was used without further purification. Sorbite anhydride monostearic acid ester (Span-85) and Tween 80 (polyoxyethylene (20) sorbitan monooleate), commercial grade, Beijing Chemical Co., China, Titanium tetrabutoxide (TTB), Darocur 1173 (2-hydroxy-2-methylpropiophenone), and trimethylolpropyltriacrylate (TMPTA), chemical grade, were used without further treatment.

Corresponding author: Yuechuan Wang, **E-mail:** gycwang@163.net

2.2. Methods

(1) Preparation of titania reverse micelles.

Span-85 and Tween 80 were first mixed in butyl acrylate and then water was added in drops to form transparent reverse micelles. Mixtures of acrylic acid and TTB were added carefully into the above reverse micelles while the solution was stirred mildly. After hydrolysis of titanium butoxide at room temperature for at least 30 min, stable and clear titania-reversed micelles were successfully obtained and used for the preparation of the hybrid films. The mass ratio was BA:TMPTA:surfactant:H_2O:TTB:AA=100:10:10:4.5:30:15.

(2) Preparation of titania-acrylic polymer hybrid films.

Photoinitiator Darocur1173 (5wt%, based on the total monomer mass) was added to the above titania-reversed micelles, and then hybrid organic-inorganic films were deposited *via* casting on the precleaned glass substrates. Photopolymerization was achieved by irradiating the samples with a high-pressure mercury lamp. After about 6 min of irradiation, the transparent hybrid films were obtained.

(3) Characterizations.

The X-ray photoelectron spectrum (XPS) was recorded on a VG ESCALABMIK II spectrometer with an Al K_α X-ray source and constant pass energy of 50 eV. The C1s peak (284.6 eV) was used as the reference for the correction of the XPS positions of the film obtained. TGA of the hybrid film was measured on a Dupont 2100 instrument. The temperature program was 10.0 K/min from 20°C to 600°C under N_2 atmosphere. Film surface morphologies were examined by atomic force microscopy (AFM) measurements using a Digital Instruments NanoScope IIIa instrument in tapping mode with a silica probe (NSC 11) and a frequency of 65 kHz.

3. Result and discussion

3.1. Preparation of titania-acrylic polymer hybrid films

The sol-gel process is a powerful method for the design of new materials based on the hydrolysis and condensation reactions of the precursor such as metal alkoxide. In the case of TTB, the overall hydrolysis and condensation reaction are described below.

$$Ti(OR)_4 + xH_2O \rightarrow Ti(OH)_x(OR)_{4-x} + xROH \quad (1)$$

$$(OR)_{4-x}(OH)_{x-1}Ti{-}OH + XO{-}Ti(OH)_x(OR)_{3-x} \rightarrow (OR)_{4-x}(OH)_{x-1}Ti{-}O{-}Ti(OR)_{3-x}(OH)_x + xOH \quad (2)$$

where R= $-(CH_2)_3CH_3$; x=H, R.

TTB is very reactive and direct hydrolysis usually produces precipitates. For these systems, direct precipitation is avoided by adding hydroxylated-complexing ligands to the titanium precursor [8] or by the confinement of water in reverse micelles [9]. As shown in Fig. 1, the hydrolysis of TTB may occur inside the reverse micelle by the penetration of Ti precursor through the surfactant layer, or in the hydrocarbon phase by reacting with water attached to the polar head of a surfactant molecule released from the reverse micelle. Condensation reactions lead to the formation of Ti–O–Ti bridge and enhance particle growth. These particles are partially hydroxylated, and the condensation reactions between them give precipitates or generate a network enclosing the liquid phase. Both processes involve the rearrangement of surfactant molecules that may either be adsorbed to the partially hydroxylated skeleton or form reverse micelles in the solution phase. Therefore, the hydrolysis and condensation reactions were controlled by the confinement of titania nanoparticles inside the reverse micelles.

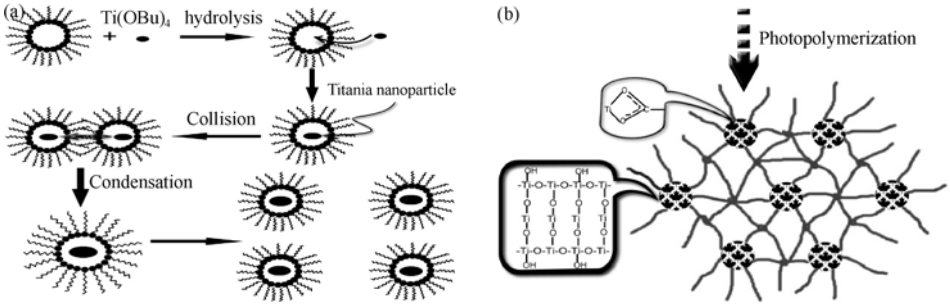

Fig. 1. Schematic illustration of the preparation of titania/acrylic polymer nanocomposites: (a) synthesis of titania-reversed micelles; (b) *in situ* photopolymerization.

Titanium alkoxides are, in fact, known to readily react with carboxylic acids such as methyl acrylic acid (MAA) [10] in a mild condition by competitive pathways: substitution (the following Eq. (3)), nonhydrolytic condensation and/or elimination of an ester (the following Eq. (4)) that generate Ti–O–Ti bonds, or by hydrolysis-condensation (Eqs. (1) and (2)) after a slow esterification (Eq. (4)).

$$Ti(OR)_4+xR'COOH\rightarrow Ti(OR)_{4-x}(R'COO)_x+xROH \quad (3)$$

$$n Ti(OR)_{4-x}(R'COO)_x\rightarrow n/2[(OR)_{3-x}Ti-O-Ti(RCOO)_{x-1}]+R'COOR \quad (4)$$

$$ROH+R'COOH\rightarrow R'COOR+H_2O \quad (5)$$

In this study, reactive monomer acrylic acid (AA) was used as the carboxylic acid ligand to further control the hydrolysis reaction and construct the chemical linkages between the organic and inorganic phases.

After the formation of stable and transparent titania-reversed micelles, a photoinitiator was added and the mixtures were irradiated using a high-pressure mercury lamp for 6 min, and finally the titania-acrylic polymer hybrid films were formed.

3.2. Effects of postthermal treatment and UV irradiation on XPS spectra

Fig. 2 shows the high-resolution XPS spectra of individual lines of Ti2p of the as-synthesized nanosized TiO_2/polyacrylates hybrid films. Samples A and B show two peaks of $Ti2p_{3/2}$ and $Ti2p_{1/2}$ at 458.5 and 464.2 eV, respectively, with a peak separation of 5.7 eV between the $Ti2p_{3/2}$ and $Ti2p_{1/2}$ peak. The value corresponds to a $Ti2p_3$ binding energy of Ti (IV) ion. However, the bonding energy located at 458.5 eV is shifted in comparison with the corresponding value at 459.2 eV for TiO_2 rutile/anatase [11-12]. Our results are consistent with other reports by Ozin [11] and Zaban groups [12]. They attributed the shift to the interaction between titania and the surfactants that had an effect on the microenvironment of titanium.

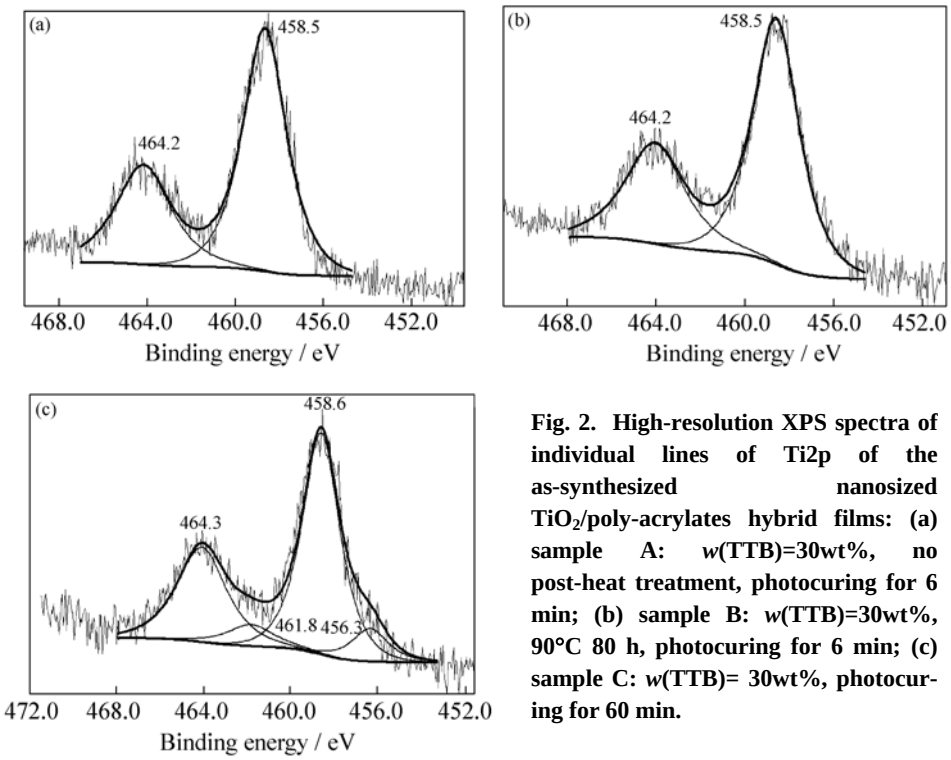

Fig. 2. High-resolution XPS spectra of individual lines of Ti2p of the as-synthesized nanosized TiO_2/poly-acrylates hybrid films: (a) sample A: *w*(TTB)=30wt%, no post-heat treatment, photocuring for 6 min; (b) sample B: *w*(TTB)=30wt%, 90°C 80 h, photocuring for 6 min; (c) sample C: *w*(TTB)= 30wt%, photocuring for 60 min.

In sample C irradiated by UV for 60 min, the two peaks located at 458.5 and 464.2 eV are assigned to the core levels of $Ti^{4+}2p_{3/2}$ and $Ti^{4+}2p_{1/2}$, respectively. After curve fitting, two additional peaks located at 456.3 and 461.8 eV ascribed to $Ti^{3+}2p_{3/2}$ and $Ti^{3+}2p_{1/2}$ could be identified, suggesting the presence of Ti^{3+} species in the irradiated sample C [13]. However, for the 6-min-UV-irradiated samples, with or without postthermal treatment, there were no additional peaks in Ti2p spectrum except for $Ti^{4+}2p_{3/2}$ and $Ti^{4+}2p_{1/2}$.

UV illumination generates Ti^{3+} defect sites on TiO_2 surface through a surface reduction process of Ti^{4+} to Ti^{3+} [14]. The Ti^{3+} defects are created by the removal of surface oxygen atoms, or bridging oxygen atoms on those particle faces and oxygen vacancies are generated on the surface. The possible reaction to induce the formation of oxygen vacancies is assumed to be the following [15]:

$$2Ti^{4+}+O^{2-}\xrightarrow{UV}(AV)+2Ti^{3+}+1/2O_2$$

where AV is anion vacanicies.

Fig. 3 shows the high-resolution XPS spectra of the O1s region for the nanosized TiO_2/polyacrylates hybrid films. The O1s region is composed of three peaks. The main peak located at 532.1 eV is attributed to the hydroxyl group of TiOH and oxygen doubly bonded to carbon (*O=C–O), as well as the peak located at 533.6 eV to oxygen singly bonded to carbon (O=C–O*) and

oxygen of water, and the minor peak located at 529.9 eV to Ti–O–Ti.

It is noted that for all the samples, no peak appears at 532.8 eV in the O1s spectrum. The binding value is consistent with the structure of C–O linkage of the alkoxide group. The result indicates complete hydrolysis of TTB during the 6-min-UV irradiation.

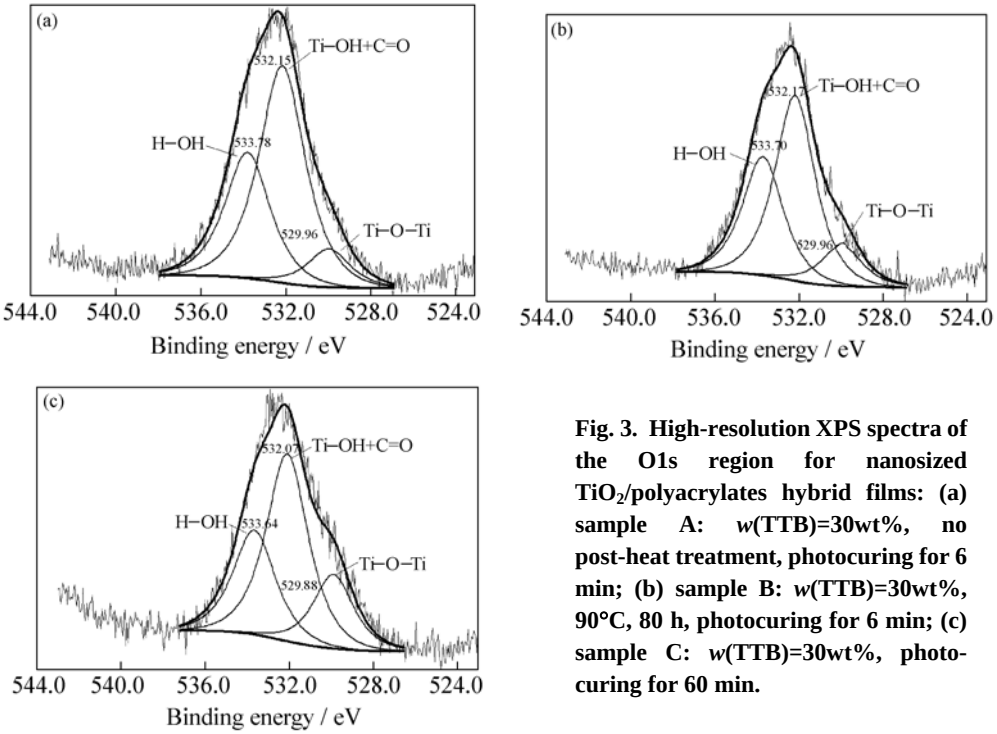

Fig. 3. High-resolution XPS spectra of the O1s region for nanosized TiO_2/polyacrylates hybrid films: (a) sample A: *w*(TTB)=30wt%, no post-heat treatment, photocuring for 6 min; (b) sample B: *w*(TTB)=30wt%, 90°C, 80 h, photocuring for 6 min; (c) sample C: *w*(TTB)=30wt%, photocuring for 60 min.

XPS reveals the quantitative information of surface composition (≤5 nm) of the hybrid films. Table 1 lists the results of curve fitting of XPS spectra for the three TiO_2 hybrid samples, where ri (%) is the ratio of each contribution to the total of both kinds of oxygen contributions, and xi (%) is the minimum molar ratio of Ti–O–Ti to TiOH in TiO_2 hybrid films on the assumption that all TTB are hydrolyzed into $Ti(OH)_4$. Therefore the molar ratio of n(COO)/ n(TiOH)≥2.695 is calculated according to the experimental compositions and the maximum content of TiOH is estimated by subtracting the *O=C–O group from the overlapping peaks at 532.1 eV.

It is seen from Table 1 that the xi values as compared with sample A increase from 0.606 to 0.940 and 1.318 for samples B and C, respectively. The only difference between them lies in the posttthermal treatment and exposure time to UV light. Therefore, the relative TiOTi content of samples A, B, and C is in the order as follows: sample C > sample B >sample A, whereas, the relative content of TiOH is in the inverse sequence. This is ascribed to the fact that exposure time to UV light and posttthermal treatment can further enhance the dehydrolyzing reaction between TiOH and the formation of TiOTi groups, with a much more remarkable influence for the former.

In the case of photocuring for as long as 60 min, water could more easily vaporize from the hybrid film by thermal effect (>100°C) released from UV light during photopolymerization. Consequently, TiOH groups at the TiO_2 surface were brought closer, which allowed in turn to complete the condensation reaction to a greater extent than in the case of photocuring for 6 min. Moreover, when excessive water was added, longer UV irradiation could promote hydroxyl groups to be effectively excited and dissociate, and form Ti–O–Ti bond [16-17].

3.3. Effects of posttthermal treatment and UV irradiation on thermal stability

The thermal stability of the titania-acrylic polymer hybrid film was evaluated using the thermal gravimetry analysis (TGA) technique at programmed heating process (10°C/min). The results are shown in Fig. 4 and Table 2. From the differential curves of TGA (DTGA), the temperature at which there is a maximum mass loss rate (T_{max}), as well as the decomposition onset temperature (T_{onset}), is considered a parameter for the estimation of the thermal stability.

As shown in Fig. 4 and Table 2, sample A (TTB=0wt%) exhibits a gradual mass loss starting from ambient temperature to 317.7°C, accompanied by a mass loss of 4.92wt% and a DTGA of 1.84wt%/min. This is mainly attributed to the removal of volatile nonreactive monomers, and shows an almost complete mass loss of about 97.03wt% and a DTGA of 4.08wt%/min up to 413.2°C.

On the contrary, sample B without posttthermal

treatment shows a $DTGA_{max}$ at 183.38°C between 133.01°C and 255.1°C, with a corresponding mass loss between 4.28wt% and 26.47wt%. This corresponds to the removal of nonreactive monomers, surfactants, 1-butanol and absorbed water in the hybrid films. However, there is little mass loss above 500°C, which indicates the almost complete decomposition of organic molecules, and the stabilization of TiO_2 in the hybrid film.

Table 1. Results of curve-fitting of the high-resolution XPS spectra for the O1s region

Sample	O1s region	E_b / eV	ri / %	xi / %
A	O1s (Ti–O–Ti)	529.9	9.48	0.606
	O1s (TiOH, C*=O–O)	532.1	57.80	
	O1s (H_2O, O=C–O*)	533.7	32.72	
	O1s (C–O)	532.8	0.00	
B	O1s (Ti–O–Ti)	529.9	14.16	0.940
	O1s (TiOH, C*=O–O)	532.1	55.68	
	O1s (H_2O, O=C–O*)	533.7	30.16	
	O1s (C–O)	532.8	0.00	
C	O1s (Ti–O–Ti)	529.8	18.68	1.318
	O1s (TiOH, C*=O–O)	532.1	52.36	
	O1s (H_2O, O=C–O*)	533.6	28.96	
	O1s (C–O)	532.8	0.00	

Note: ri (%) is the ratio of each contribution to the total of both kinds of oxygen contributions; xi is the minimum amount ratio of Ti–O–Ti to TiOH in the same sample. Sample A: *w*(TTB) = 30 wt%, room temperature, photocuring for 6 min; Sample B: *w*(TTB) = 30 wt%, 90°C, 80 h, photocuring for 6 min; Sample C: *w*(TTB)= 30 wt%, photocuring for 60 min.

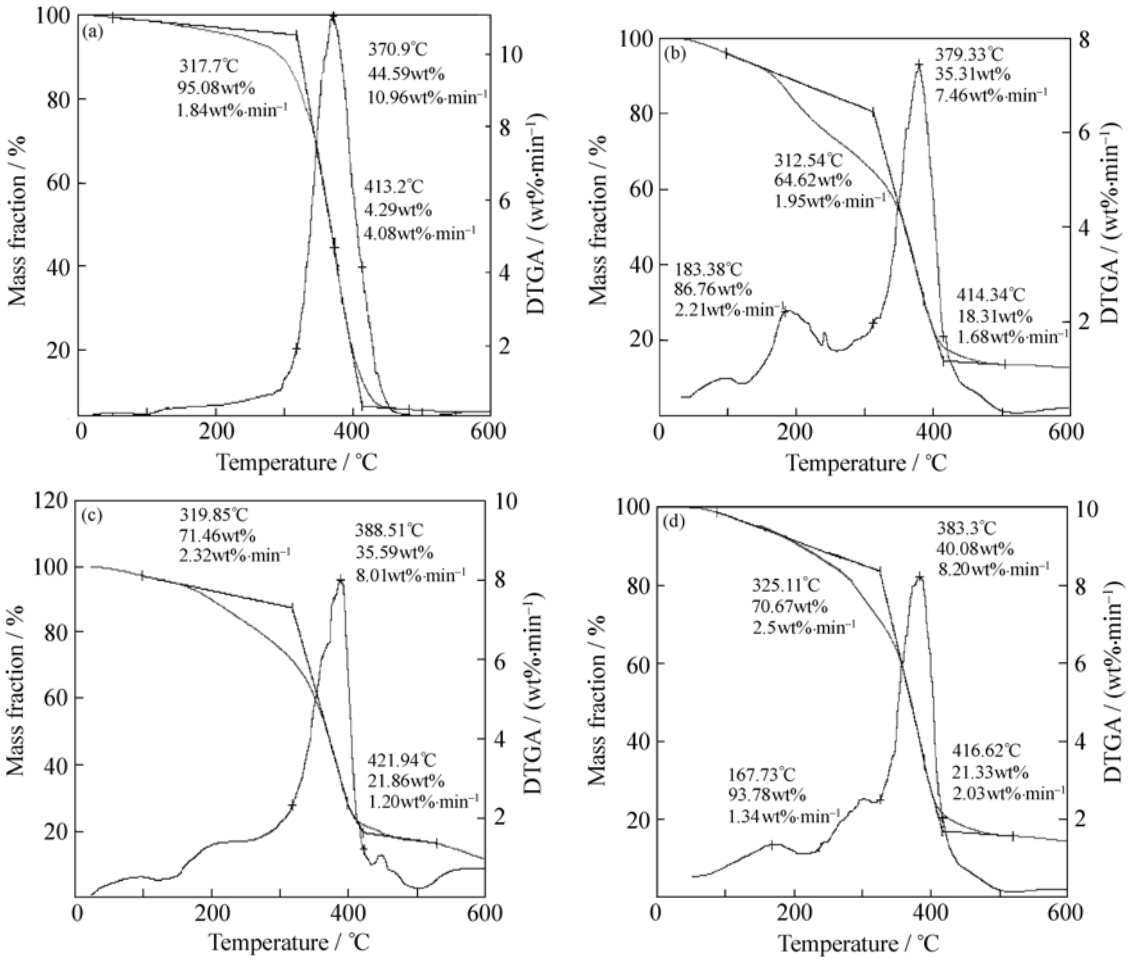

Fig. 4. TGA and DTGA curves of the hybrid films as a function of irradiation and postthermal treatment: (a) sample A: *w*(TTB)TTB = 0 wt%, pure polyacrylates without surfactant and water; (b) sample B: *w*(TTB) = 30 wt%, room temperature, photocuring for 6 min; (c) sample C: *w*(TTB) = 30 wt%, 90°C, 80 h, photocuring for 6 min; (d) sample D: *w*(TTB) = 30 wt%, photocuring for 60 min.

Table 2. TGA and DTGA data of the TiO_2-PBA hybrid films

Sample	T_{onset} / °C	T_{max} / °C	Residue at T_{max} / wt%	DTGA at T_{max} / (wt%·min^{-1})
A	317.70	370.90	44.59	10.96
B	312.54	379.33	35.31	7.46
C	317.85	388.51	35.59	8.01
D	325.11	383.30	40.08	8.20

Note: sample A: *w*(TTB) = 0 wt%, pure polyacrylates without surfactant and water; sample B: *w*(TTB) = 30 wt%, room temperature, photocuring for 6 min; sample C: *w*(TTB) = 30 wt%, 90°C, 80 h, photocuring for 6 min; sample D: *w*(TTB) = 30 wt%, photocuring for 60 min.

It is noted that an enhanced thermal stability of the hybrid films is achieved by way of postthermal treatment and prolonged exposure to UV light. As shown in Table 2, T_{onset} of samples C and D, as compared with that of sample A, increases from 317.7°C to 319.85°C and 325.11°C, respectively, and T_{max} of samples C and D increases from 370.9°C to 388.51°C and 383.3°C, respectively.

Except for the hybrid films without postthermal treatment, all the other titania-acrylic polymer hybrid materials have an enhanced decomposition onset temperature, as compared with sample A. As shown in Table 2, T_{onset} of the organic polymer of sample B (312.54°C) is a little lower than that of sample A (317.7°C). This is ascribed to the removal of water and 1-butanol released from the hydrolysis of TTB, and therefore results in a larger slope of the TGA curve of sample B within the initial temperature than that of sample A, without removal of water and 1-butanol.

Obviously, the titania-acrylic hybrid films can upgrade T_{onset} and T_{max}. This is because the inorganic particles restrain the movement of the polymer chain segment; therefore, it needs much more energy to decompose the organic chains.

3.4. AFM study

AFM phase images of the samples with 6-min-irradiation are shown in Figs. 5-6. The bright and dark regions of the AFM phase images of the hybrid film correspond to the inorganic domain and organic domain, respectively. The AFM phase images show that the phase morphologies of the hybrid films are closely correlated to the postthermal treatment. The AFM micrographs of the hybrid films with and without postthermal treatment show the presence of inorganic domains with a mean size of 28.84 and 25.26 nm, respectively. This demonstrates that the inorganic domain size is related to the postthermal treatment.

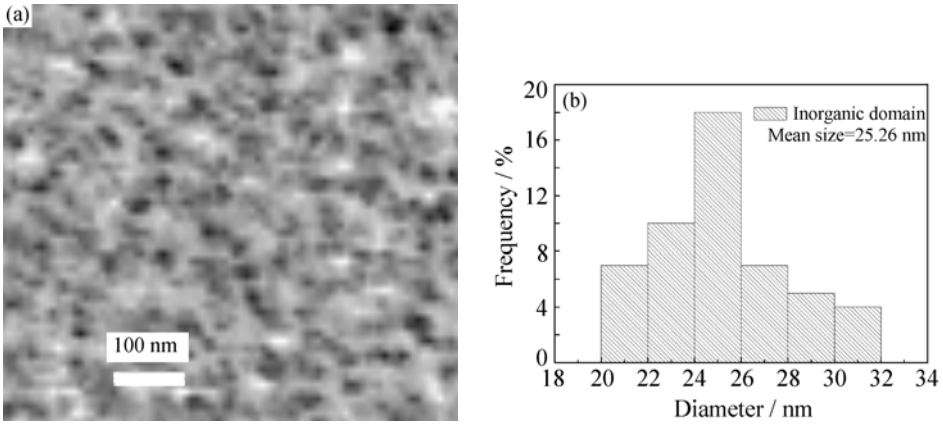

Fig. 5. AFM phase diagram of the titania-acrylic polymer hybrid film (a) and the histogram of inorganic domains of the hybrid film (b) (*w*(TTB)=30wt%, non-postthermal treatment, photocuring for 6 min).

Moreover, AFM phase images of the samples with 6-min irradiation indicate noncontinuous inorganic domains. However, the AFM phase image of the sample with 60-min irradiation, as shown in Fig. 7, indicates continuous inorganic domains. This may be ascribed to inorganic particle aggregation caused by surfactant desorption from the TiO_2 particles as a result of the tremendous heat released from the infrared irradiation during UV irradiation for as long as 60 min.

Overall, the AFM phase images show that the inorganic domains with a mean size of 21.57-28.84 nm, were uniformly dispersed in the polymeric networks. Therefore, the new preparation method of titania-acrylic polymer hybrid films by sol-gel process in reverse micelles and subsequent *in situ* photopolymerization was effective.

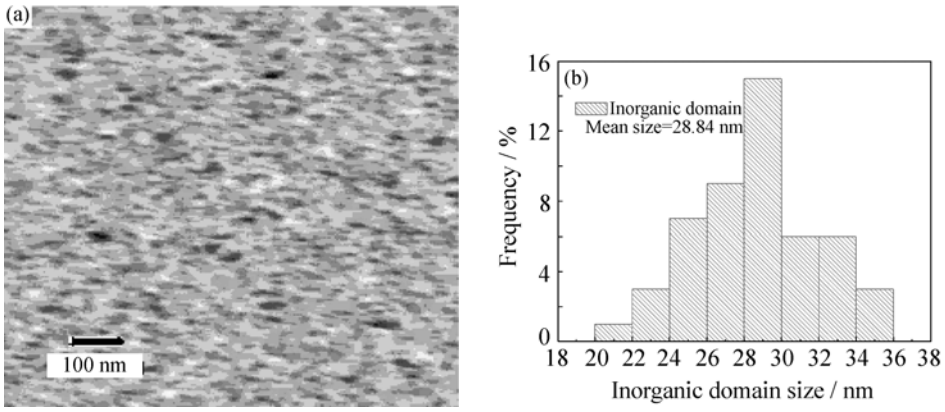

Fig. 6. AFM phase diagram of the TiO_2/polyacrylates film with postheat treatment (a) and the histogram of inorganic domains of the hybrid film (b) (*w*(TTB)=30wt%, photocuring for 6 min, postheat treatment: 90°C, 80 h).

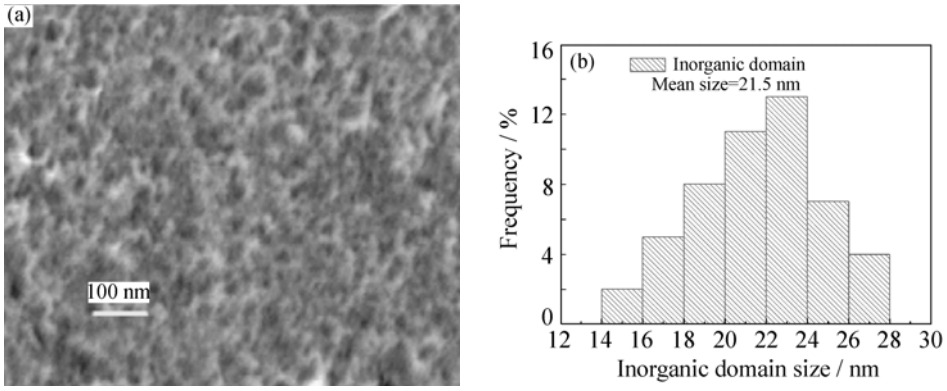

Fig. 7. AFM phase diagram of the TiO_2/polyacrylates film with photocuring for 60 min (a) and the histogram of inorganic domains of the hybrid film (b) (*w*(TTB)=30wt%).

4. Conclusions

UV curable, transparent acrylic resin/titania organic-inorganic hybrid films were prepared by controlled hydrolysis of titanium tetrabutoxide (TTB) in Span85/Tweeen80 reverse micelles and subsequent *in situ* photopolymerization of acrylic monomers. The titania-acrylic polymer films can upgrade the decomposition onset temperature as well as the temperatures at which there is a maximum mass loss rate (T_{max}). XPS data suggested that the prolongation of irradiation time and the postthermal treatment promoted titania formation, with the former showing a more remarkable influence. TGA data show that TiO_2-hybrid films can upgrade the decomposition onset temperature (T_{onset}) and the temperature at which there is a maximum mass loss rate (T_{max}). AFM images show that the hybrid films have characteristics of homogeneous distribution of the inorganic phases in a nanosized scale within the polymer matrix.

Acknowledgments

The authors gratefully acknowledge the fruitful discussion with Prof. Yong Zhang of Chengdu University of Technology on the preparation of nanosized TiO_2.They are also grateful to Yi Yuan and Wenqiong He of Chengdu University of Technology for rendering all possible facilities.

References

[1] P.N. Sreekumari, T. Radhakrishnan, N. Revaprasadu, *et al*., Structure and properties of PbS-polyacrylamide nanocomposites, *Appl. Phys. A*, 81(2005), No.4, p.835.

[2] T. Smirnova, O. Sakhno, and V. Bezrodnyj, Nonlinear diffraction in gratings based on polymer-dispersed TiO_2/ nanoparticles, *Appl. Phys. B*, 80(2005), No.8, p.947.

[3] T.I. Izaak, O.V. Babkina, and G.M. Mokrousov, Morphology, texture, and properties of products obtained by annealing of porous silver-polyacrylate nanocomposites, *Tech. Phys.*, 50(2005), No.5, p.669.

[4] P.B. Bhimaraj, L.A. David, W. Gregory, *et al*., Effect of matrix morphology on the wear and friction behavior of alumina nanoparticle/poly(ethylene) terephthalate composites, *Wear*, 258(2005), No.9, p.1437.

[5] B. Wang, G.L. Wilkes, J.C. Hedrick, *et al*., New high refractive index organic/inorganic hybrid materials from sol-gel processing, *Macromolecules*, 24(1991), p.3449.

[6] L.H. Lee and W.C. Chen, High refractive index thin films prepared from trialkoxysilane-capped poly (methyl methacrylate)-titania hybrid materials, *Chem. Mater*., 13(2001), p.1137.

[7] S. Hiroyo, T. Kanayo, A. Yasuhiko, *et al*., Patterning of hybrid titania film using photopolymerization, *Thin Solid Films*, 466(2004), p.48.

[8] J. Blanchard, S. Barboux-Doeuff, J. Maquet, and C. Sanchez, Investigation of hydrolysis-condensation reactions of titanium (IV) butoxide precursors, *New J. Chem*., 19(1995), p.929.

[9] N. Francois, B. Ginzberg, and S.A. Bilmes, Parameters involved in the sol-gel transition of titania in reverse micelles, *J. Sol Gel Sci. Technol*., 13(1998), p. 341.

[10] U. Schubert, N. Hüsing, and A. Lorenz, Hybrid inorganic-organic materials by sol-gel processing of organofunctional metal alkoxides, *Chem. Mater*., 7(1995), p.2010.

[11] D. Khushalani, G.A. Ozin, and A. Kuperman, Glycometallate surfactants, Part 2: Nonaqueous synthesis of mesoporous titanium, zirconium and niobium oxides, *J. Mater. Chem*., 1999, 9, 1491.

[12] Y.Q. Wang, S.G. Chen, X.H. Tang, O. Palchik, A. Zaban, *et al*., Mesoporous titanium dioxide: sonochemical synthesis and application in dye-sensitized solar cells, *J. Mater. Chem*., 11(2001), p.521

[13] A.N. Shultz, W. Jang, M. Hetherington, *et al*., Comparative second harmonic generation and X-ray photoelectron spectroscopy studies of the UV creation and O_2 healing of Ti^{3+} defects on (110) rutile TiO_2 surfaces, *Surf. Sci.*, 339(1995), p.114.

[14] R. Wang, K. Hashimoto, A. Fujishima, *et al*., Photogeneration of highly amphiphilic TiO_2 surfaces, *Adv. Mater*., 10(1998), p.135.

[15] R.D Shannon and J.A. Pask, Kinetics of the anatase-rutile transformation, *J. Am. Ceram. Soc*., 48(1965), p.391.

[16] K. Shimizu, H. Imai, H. Hirashima, *et al*., Low-temperature synthesis of anatase thin films on glass and organic substrates by direct deposition from aqueous solutions, *Thin Solid Films*, 351(1999), p.220.

[17] H. Imai and H. Hirashima, Alternative modification methods for sol-gel coatings of silica, titania and silica-titania using ultraviolet irradiation and water vapor, *Thin Solid Films*, 351(1999), p.91.